Peer reviewed version

Link to published version (if available):
10.1016/j.compositesb.2018.05.019

Link to publication record in Explore Bristol Research
PDF-document

University of Bristol - Explore Bristol Research
General rights

Hybrid bio-composites reinforced with sisal-glass fibres and Portland cement particles: A statistical approach

Sergio Luiz Moni Ribeiro Filho[1], Pablo Resende Oliveira[1], Luciano Machado Gomes Vieira[1], Tulio Hallak Panzera[1*], Rodrigo Teixeira Santos Freire[2], Fabrizio Scarpa[3]

[1]Centre for Innovation and Technology in Composite Materials - CIT^{e}C, Department of Mechanical Engineering, Federal University of São João del Rei - UFSJ, São João del Rei, Minas Gerais, Brazil. *Corresponding author: panzera@ufsj.edu.br

[2]Centre for Innovation and Technology in Composite Materials - CIT^{e}C, Department of Natural Science, Federal University of São João del Rei - UFSJ, São João del Rei, Minas Gerais, Brazil.

[3]Bristol Composites Institute (ACCIS), University of Bristol, BS8 1TR Bristol, UK.

ABSTRACT: *The hybrid configuration of bio-reinforced composites has established a new extended boundary for the development of pro-ecological technologies due to light weight, moderate specific strength, low cost, environmental benefits, and potential applications of natural components. This work investigates the physical and mechanical properties of hybrid composites made of sisal/glass fibres and Portland cement inclusions. A full factorial design was generated to identify the effects of the stacking sequence and cement particles on the flexural strength, flexural stiffness, apparent density, apparent porosity and water absorption of the composites. The significant contributions of these main factors and their interactions were determined via Design of Experiments (DoE) and Analysis of Variance (ANOVA). The fracture features and damage mechanisms of hybrid composite were also reported. The inclusion of cement microparticles led to an increased apparent porosity, as well as enhanced water absorption, flexural stiffness and flexural strength of the hybrid composites. The mechanical properties were strongly dependent on the fibre stacking sequence, which accounts for approximately 98% of the effects observed. Moreover, the stacking sequence affected the damage mechanism of the bio-composites. Finally, the replacement of glass fibres by unidirectional sisal reinforcements may potentially improve the specific properties in structural applications with an environmental sustainable footprint.*
Keywords: *Hybrid composites; biomaterials; fibres; mechanical properties; microscopy.*

1. Introduction

During recent years, new techniques of cultivation, extraction and processing of natural fibres have allowed the development of new classes of sustainable composites derived from renewable sources [1-2]. In particular, hybrid bio-reinforced composites based on the use of natural and glass fibres have gained some traction in structural design for a range of different applications [3-4].

Hybrid composites are multifunctional materials that consist of two or more distinct reinforcement phases and combined in the same matrix. The reinforcements can include two types of individual fibres, or a combination of fibres and multiscale particles.

Hybrid synthetic fibre composites have shown an enhanced mechanical behaviour when ceramic particles are incorporated [5-8]. Santos *et al.* [9] have studied the incorporation of 1wt%, 2wt% and 3.5wt% of silica particles in glass fibre reinforced composites and observed that ceramic particle reinforcements tend generally to increase the tensile modulus (at 1wt%), the flexural modulus (at 3.5wt%) and reduce the tensile and flexural strength of these composites. Detomi *et al.* [10] have shown that the inclusion of silica and silicon carbide microparticles increases the stiffness of glass fibre reinforced composites. The improvement of the mechanical properties has been attributed not only to the interlocking effect at the interlaminar region favoured by the particles, but also to the increase of the stiffness of the matrix phase [11]. Enhancements in thermal stability [12], tribological performance (wear and friction) [13], mechanical shear strength and impact of composites [14] can also be obtained by the inclusions of particles in polymeric composites.

In general, natural fibres are considered as a potential replacement to synthetic ones, mainly of glass type [15]. The use of natural fibres as reinforcements has been remarkably promising economically as well as in terms of improved environmental impact [16]. Natural fibres can be considered as natural aggregates of cellulose, hemicellulose and lignin, with smaller amounts of free sugars, proteins, extractives and inorganic products. The sisal plant (*Agave sisalana*) can produce between 200 and 250 leaves before flowering. Each leaf can reach from 60 up to 100 mm in width, and from 1500 to 2000 mm in length. Each leaf contains approximately 700 to 1400 bundles of fibres, whose length can vary from 0.5 to 1.0 m [1-2]. In general, the sisal leaf is composed by approximately 4% of fibres, 1% of superficial film (cuticle), 8% of dry matter and 87% of water [17]. These constituents, except for the fibres, are considered as residues

originated from the processing, used as organic fertilizers, animal feed and in the pharmaceutical industry [18]. Angrizani *et al.* [19] have stated that sisal fibres could have their added-value multiplied if used as reinforcements in polymeric composites. Sisal fibres are lightweight, non-toxic, present high tensile specific modulus and strength, and excellent thermal and acoustic insulation properties. Moreover, sisal causes less abrasion damage to moulding equipment and costs about ten times less than glass fibres. In addition, sisal fibres can be easily surface modified, which enhances fibre-matrix adhesion [20].

The mechanical efficiency of natural fibre reinforced composites can be improved even further via hybridization, i.e., by combining synthetic and natural fibres in the same composite [3]. Hybrid composite designs can provide flexibility, high life cycle properties, low cost and sustainable characteristics [3-4, 21]. Recent publications have been addressed to hybrid composites of sisal and glass fibres. Padanattil *et al.* [22] investigated hybrid composites reinforced with sisal and glass fibres as a potential choice for the retrofitting of reinforced concreted structures. KC *et al.* [23] analysed the influence of injection moulding processing parameters of two sisal-glass fibre composites with different contents using the Taguchi Method. Aslan *et al.* [24] evaluated the tribological and mechanical responses of sisal/carbon and sisal/glass hybrid fibre reinforced polypropylene (PP) composites.

The incorporation of Portland cement into sisal short fibre reinforced composites was investigated by Santos *et al.* [25], who reported an increase in water absorption, damping ratio and flexural modulus. Higher stiffness was obtained when 10wt% of cement microparticles were added. The mechanical behaviour of hybrid glass fibre reinforced composites with cement inclusion was also investigated by Melo *et al.* [26] and Torres *et al.* [27]. Melo *et al.* [26] reported improved flexural properties when cement microparticles were added on the upper beam side (under compression) of the glass fibre laminate. Torres *et al.* [27] also observed increased flexural stiffness when silica or cement inclusions were incorporated into the upper beam side of unidirectional glass fibre composites. Moreover, the flexural strength and impact resistance were increased when 5wt% of cement or silica particles were inserted.

This work focuses on the development of novel hybrid composites reinforced with sisal-glass fibres and Portland cement particles as an alternative substitute for glass fibre composites generally used in aircraft, automotive and building applications. This is, to the best of these authors' knowledge, the first attempt to identify the effects of Portland

3

cement on the physical and mechanical properties of hybrid composites containing unidirectional sisal and glass fibres. The cement inclusions and the stacking sequence factors were investigated using a statistical methodology based on the Design of Experiments (DoE) approach.

2. MATERIALS AND METHODS

2.1 Hybrid laminates

The hybrid bio-composites are made of epoxy polymer (RenLam M-1 and Hardener HY 951) supplied by Huntsman (Brazil), unidirectional sisal fibres sourced by Sisal Sul (Brazil), glass fibre fabric (cross ply, 200g/m^2) and Portland cement particles (Holcim-Brazil).

The sisal fibres are washed with distilled water at 80ºC for 1h and oven-dried at 50ºC until they reach a constant mass. Sisal fibres with no visible damage and a fibre length of 1 meter have then been selected. The fibres are then pre-tensioned along the longitudinal direction (0°) using a metallic mould. The manual weaving of the sisal fibre starts with a knot at the edge of the metallic structure, followed by the joining of the fibres by another knot (Figure 1). The knot is made at the ends of the metallic mould, ensuring that the working area remains without defects caused by the manufacturing process.
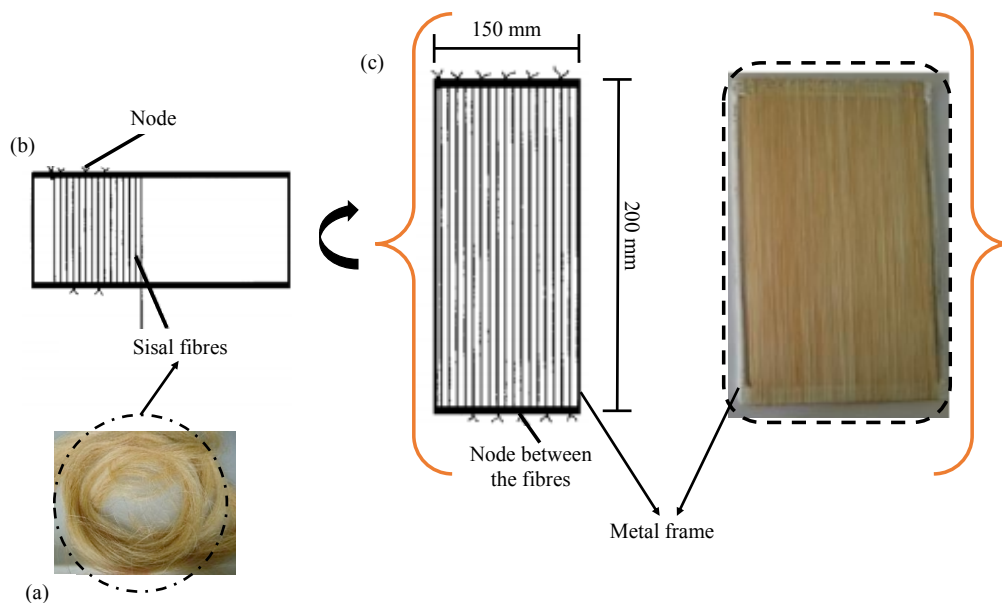

Figure 1. Sisal fibres weaving: (a) natural sisal fibres, (b) manual aligning procedure of the fibres and (c) aligned unidirectional (0º) fibres.

Preliminary tests have been performed to determine the optimized fibre-matrix mass fraction and ensure an adequate superficial finishing of the composites. Based on these tests, a fibre-matrix mass fraction of 30/70 was used to manufacture the laminated composites by hand lay-up. The sisal fibre interspacing was selected so as to approximately obtain the same grammage of the glass fibre fabric (200 g/m²). A fibre-matrix *mass* fraction is chosen instead of a more classic *volume* fraction, due to the large variability of the density of sisal fibres.

Hybrid laminates have a five-layer architecture considering the stacking sequence of sisal/glass and glass/sisal. This configuration was considered to evaluate mainly the effect of the glass fibre layer position on the flexural stiffness of hybrid composites. Two reference conditions consisting of 5 layers of [0/90°] cross-ply glass fibres and 5 layers of unidirectional sisal fibres were also fabricated to complete the stacking sequence levels. The sisal fibres are unidirectionally disposed at 0° along the direction of the sample length. Sisal fibres are generally thicker than glass fibres. Therefore, the sisal fibre layer was thicker than the glass fibre one, even though 3 unidirectional sisal laminae and 4 cross-ply glass fibre laminae have been used. Specific details of the sisal/glass and glass/sisal fibre stacking sequences are shown in Figure 2. The laminate composites are compacted by applying a force of 5N for 10h, and then cured at room temperature (20°C) for 7 days. The resulting hybrid composites have a mean thickness of 1 millimetre.
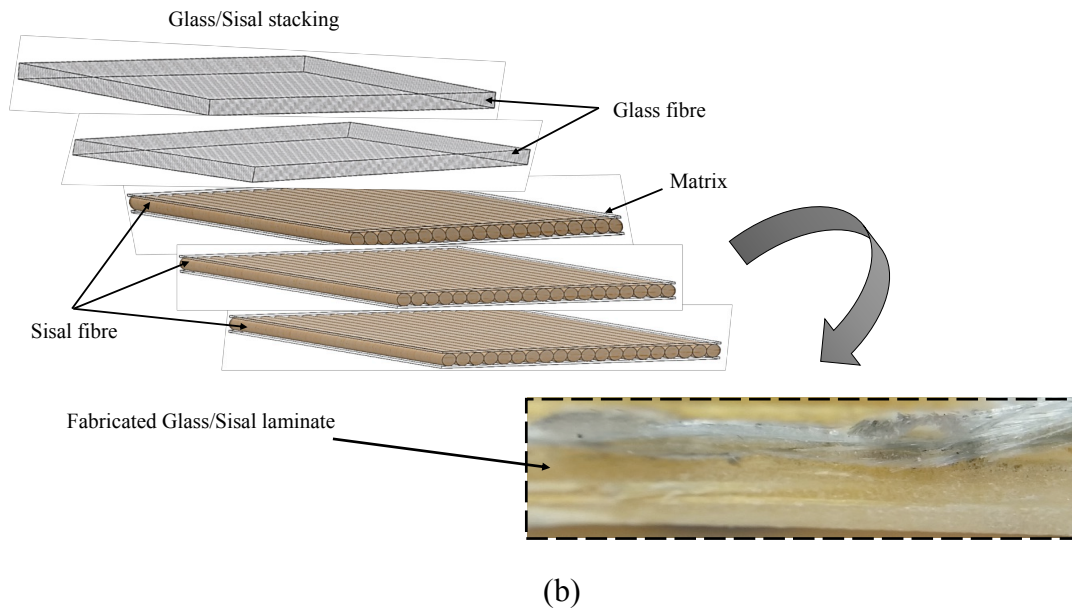

(a)

(b)
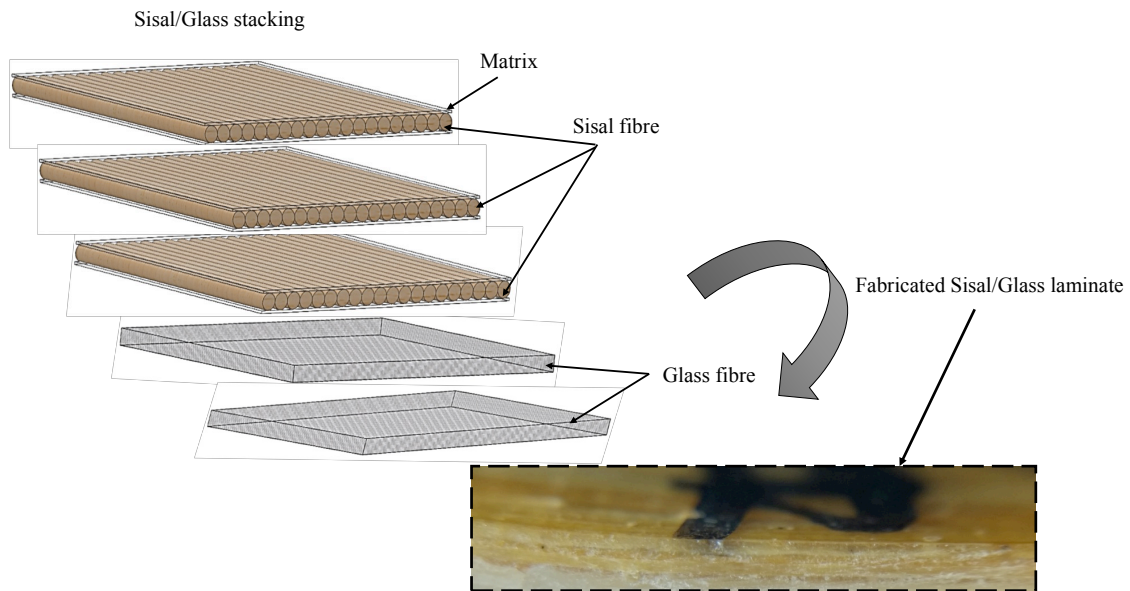
Figure 2. Sisal/Glass (a) and Glass/Sisal (b) hybrid biocomposites.

ASTM-III type Portland cement at 10wt% is used as the disperse phase in the first two top layers of the laminates. The cement particles are classified by following a sieving process at 200-325 US-Tyler. A previous investigation has been conducted by adding 2.5wt%, 5wt% and 10wt% of cement particles into the epoxy matrix phase; this study has shown that the best mechanical properties can be reached by using 10wt% of particles, hence the weight fraction used in this work [28].

2.2 Experimental design

The Full Factorial Design is a methodology that makes use of different statistical techniques to provide a structured method for planning, executing and analysing experiments [29]. DoE is also essential to identify which factors and parameters are most significant to the global mechanical and physical properties of the composites [5, 9-10,12, 20, 25].

ANOVA (analysis of variance) is used here to verify if the effect of the main factors and interaction of factors are statistically significant. In this work, ANOVA could detect how the physical and flexural properties of the composite are affected by looking at the P-Values related to the main factors and the interactions of factors. A P-value lower or equal to 0.05 (α-level of 0.05) indicates a significant effect provided by the main factors, or the presence of the interaction of factors on the response variables within a confidence interval of 95%. The main factor is only interpreted individually when there is no evidence that it interacts with the other factors [29-30]. The Anderson-Darling normality test is also performed to examine and identify whether the residual of the response

6

variables follow a normal distribution. If the P-value for the Anderson-Darling test is higher than 0.05 (i.e., an α-level of 0.05), the data follow a normal distribution, therefore validating the results of the ANOVA model [29]. ANOVA results can also indicate the influence of each factor over the responses and reveal that some of the factor-level means are different, but it does not identify which means are different. Therefore, the Tukey's multiple comparison method is also performed to extend the confidence level for each individual level. In this way, the Tukey test is used to compare the experimental levels as a grouping of treatment. The Tukey results are illustrated by using main effect and interaction plots, and by attributing letters to the factor levels. The different letters attributed to each level indicate significantly different means, whereas same letters reveal treatments with equivalent means [30].

A full factorial design $2^1 4^1$ was used to investigate the effect of the stacking sequence (sisal, glass, sisal/glass and glass/sisal) and the inclusion of cement microparticles (0wt% and 10wt%) on the mechanical and physical properties of the hybrid laminated composites. By using twelve (12) samples for each experimental condition and 2 replicates, a total of 192 samples have been produced. Table 1 shows the experimental matrix planning.

Table 1. Matrix planning.

Factors	Experimental levels
Stacking Sequence	Only Sisal Fibres
	Only Glass Fibres
	Sisal/Glass (see Figure 2.a)
	Glass/Sisal (see Figure 2.b)
Cement particle mass fraction[wt%]	0
	10

2.3 Experimental trials

The mechanical characterisation has been performed by using a Shimadzu universal testing machine (AG-X model) with a load cell of 100 kN. Three-point static bending tests have been carried out following the ASTM D790 standard [31], with a cross-head velocity of 1 mm/min. The tests have been performed at room temperature (~21°C) and at a humidity level of 58%.

The apparent density has been determined following the ASTM D792 protocol [32] by using a vacuum saturation method with distilled water at 19°C and a precision scale of 0.0001g. The apparent density (ρ_a) can be calculated as:

$$\rho_a = \frac{W_1}{Vi} \tag{1}$$

In Equation 1, ρ_a is the apparent density (kg/m³), W_1 is the dry mass of the laminate (kg) and V_i is the volume of the laminate (m³). The volume V_i can be determined by considering the density of water as 1000 kg/m³:

$$V_i = \frac{W_1 - W_3}{1000} \tag{2}$$

In Equation (2), W_3 is the mass of the laminate fully submerged in water (kg). The apparent porosity (P_a) was obtained by the Archimedes principle, using also the vacuum saturation method based on the British Standard BS 10545-3 [33]. The apparent porosity is the ratio between the volume of open pores and the volume of the impermeable portion of the sample. The equation 3 establishes the apparent porosity as a function of the dry mass of the laminate (W_1), the mass of the laminate saturated with water (W_2) and the mass of laminate fully submerged in water (W_3):

$$Pa = \frac{W_2 - W_1}{W_2 - W_3} \times 100 \tag{3}$$

The water absorption A_b was obtained from the percentage of the water absorbed by a specimen after immersion in water under vacuum, following the recommendations of the British Standard BS 10545-3- 1997 [33]:

$$A_b = \frac{W_2 - W_1}{W_1} \times 100 \tag{4}$$

3. RESULTS

The Analysis of Variance (ANOVA) and Design of Experiment (DoE) methodologies were carried out using the Minitab 16 statistical software. The P-values underlined in Table 2 indicate the significant factors and/or interactions influencing the response variables, while the values in bold represent the main effects or interactions that will be analysed via effect plots.

Table 2. Analysis of Variance (ANOVA)

Mechanical properties	
Main factor and interactions	**Full factorial design $2^1 4^1 = 8$**
	P-value ≤ 0.05

	Flexural modulus (GPa)		Flexural Strength (MPa)	
	Contribution	P-value	Contribution	P-value
Stacking Sequence	97.01%	**0.000**	99.86%	0.000
Cement Particles (%)	2.80%	**0.000**	0.01%	0.019
Stacking*Cement Particles	0.11%	0.052	0.11%	**0.000**
R² (adj)	99.76%		99.89%	
Anderson-Darling test	0.07 (P-value > 0.05)		0.06 (P-value > 0.05)	

Physical properties

Main factor and interactions	**Full factorial design $2^1 4^1 = 8$**					
	P-value ≤ 0.05					
	Apparent Porosity (%)		Apparent density (kg/m³)		Water absorption [%]	
	Contribution	P-value	Contribution	P-value	Contribution	P-value
Stacking Sequence	54.25%	0.000	99.61%	0.000	69.91%	0.000
Cement Particles (%)	17.78%	0.000	0.21%	0.000	13.27%	0.000
Stacking*Cement Particles	26.33%	**0.000**	0.14%	**0.009**	16.20%	**0.000**
R² (adj)	96.91%		99.91%		98.84%	
Anderson-Darling test	0.272 (P-value > 0.05)		0.055 (P-value > 0.05)		0.409 (P-value > 0.05)	

The value of 'R² adjusted' of Table 2 show how well the model can predict the responses for new observations. In this context, the value 'R²' corresponds to the changes of observed response values that can be attributed by controllable factors and their interactions. A 'R² coefficient' value closer to 1 (or 100%) suggests models of greater predictability. The ANOVA also determine the significant contribution of the factors and interactions at influencing the responses.

Figures 3 to 8 show the results related to grouping treatments obtained by the Tukey's multiple comparison test. The letters for each factor are indicated near the mean values for each level in the plot. When an interaction plot is presented, the Tukey's test is also performed for each level of the interacting factor.

3.1 Apparent density

The apparent density varies from 1.243 g/cm³ to 1.790 g/cm³. A second order interaction between the stacking sequence and the cement particles dispersions is significant, with a P-value of 0.009 (see Table 2). Figure 3 shows the interaction effect plot related to the mean apparent density response. The inclusion of 10wt% of particles into the hybrid stacking sequence leads to an increase of the apparent density. Glass fibre

9

laminates indeed possess higher density, when compared to sisal fibre laminates, and this is due to the higher density of glass fibre ~2.65 g/cm³ [9] against the~1.45 g/cm³ of sisal fibres [25]. Therefore, the sisal/glass and glass/sisal stacks have similar density values (letter group B).
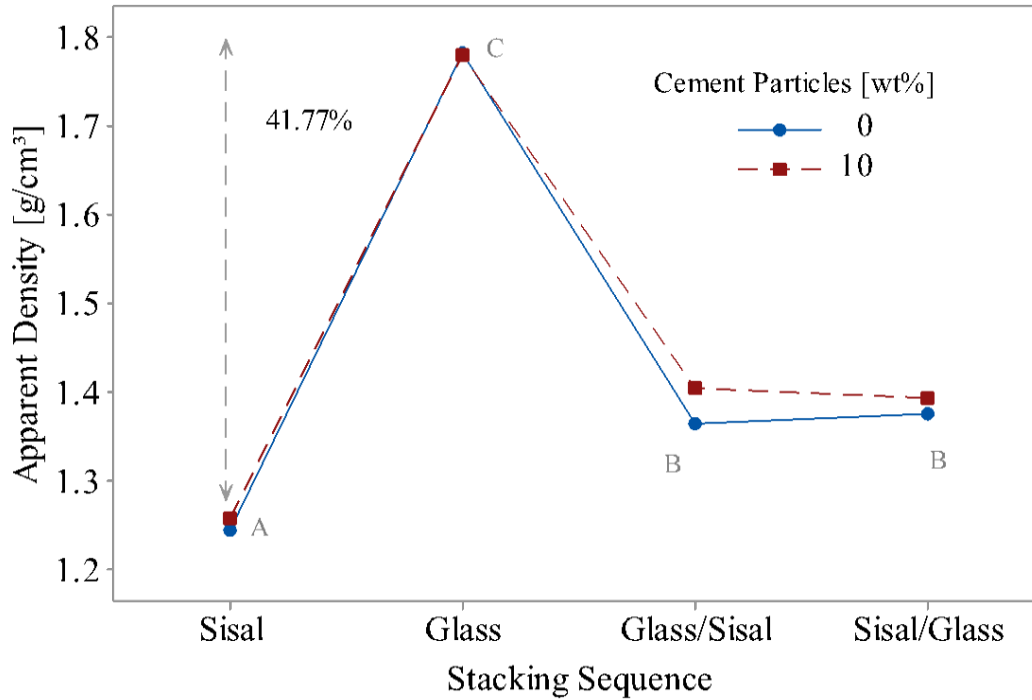

Figure 3. Interaction effect plot for the mean apparent density.

3.2 Apparent Porosity

The apparent porosity ranges between 15.3% and 25%. A second order effect is significant, as shown in Table 2. The incorporation of cement microparticles leads to an increased apparent porosity owing to the formation of micro-voids at the interfacial transition zone (ITZ). A possible hydration of the cement grains when mixed with epoxy polymer may also affect this behaviour. Panzera *et al.* [34] and Martuscelli *et al.* [35] have considered evidence of chemical interaction between Portland cement and epoxides with formation of epoxy-portlandite hydrogen bonds. Soles and Yee [36] have also reported that water molecules can penetrate the structure of the epoxy polymer through a network of nanopores, which contributes to the formation of epoxy and Portland cement interaction bonds. The glass/sisal stacking sequence also helps to generate higher levels of porosity when compared to the sisal/glass composites, and this could be explained by some uncontrolled spreading of the matrix during the manufacturing process.
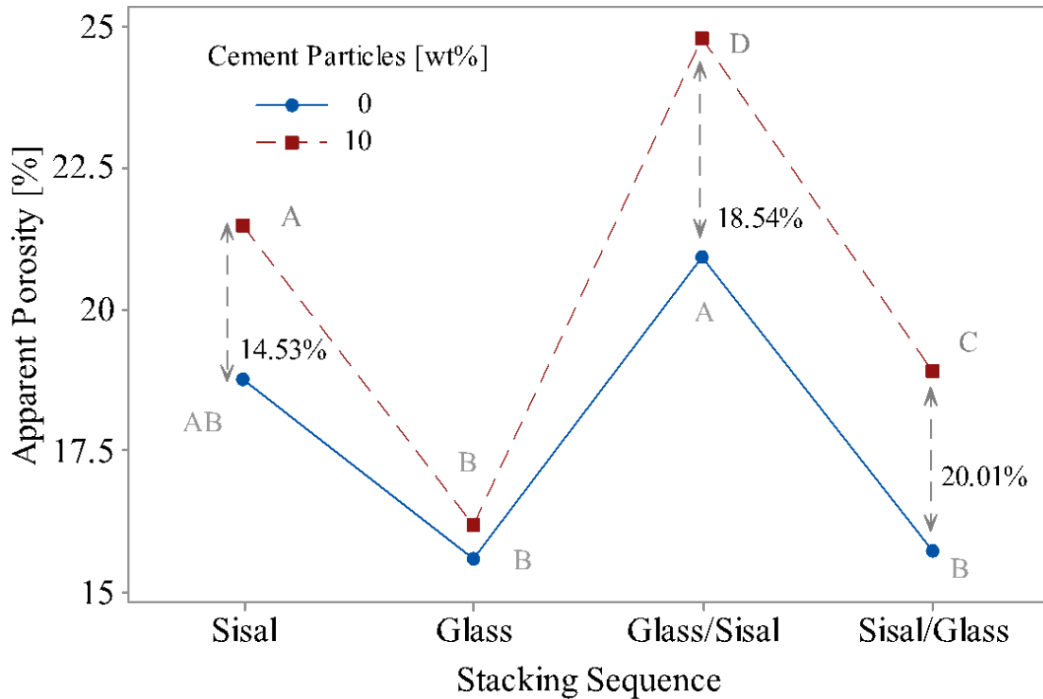
10

Figure 4. Interaction effect plot for the mean apparent porosity.

3.3 Water absorption

The water absorption, which varies from 10.5% to 22.3%, is significantly affected by the 'Stacking Sequence-Cement Particles' second-order interaction, with a P-value of 0.000 (Table 2). Figure 5 shows the interaction effect 'Stacking Sequence*Cement Particles' related to the mean water absorption. As previously discussed, the incorporation of 10wt% cement grains in the epoxy matrix not only increases the apparent porosity, but also the water absorption, except for the glass fibre-reinforced composites. This behaviour can be attributed to the larger water percolation through the cellular structure of the sisal fibres. The cement particles can therefore absorb a larger amount of water when combined with sisal fibres, instead of synthetic ones.
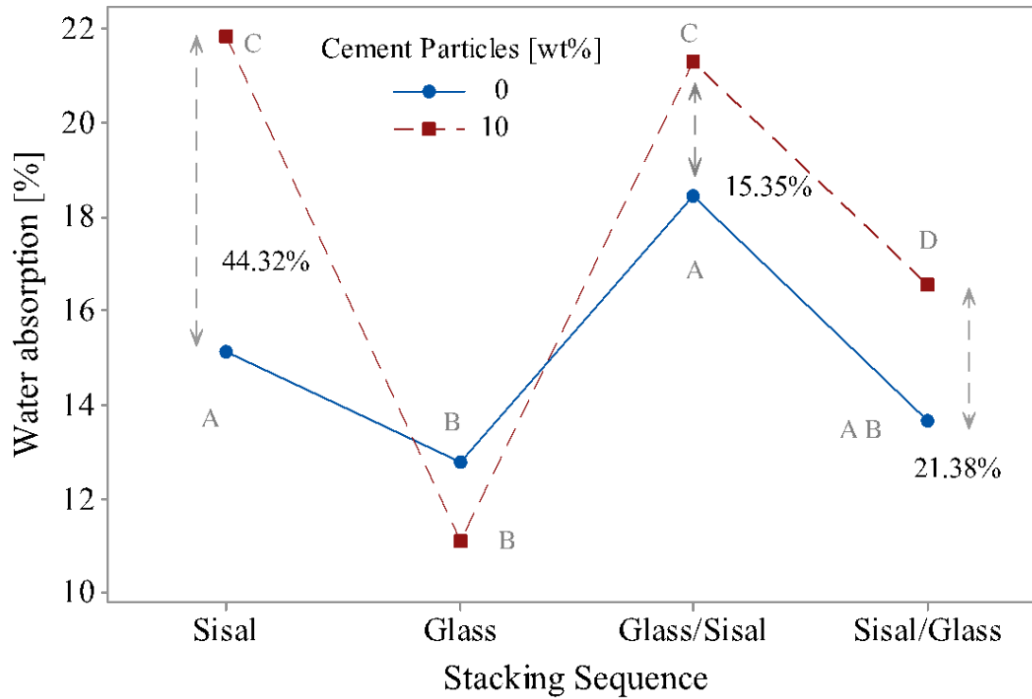
Figure 5. Interaction effect plot for the mean water absorption.

3.4 Flexural modulus

The modulus of elasticity of the hybrid composites varies from 3.84 GPa to 10.3 GPa. Only the main factors 'Stacking Sequence' and 'Cement Particles' show a relevant effect on the elastic modulus, with P-values lower than 0.05 (Table 2). The most important effect on the flexural modulus is the stacking sequence, with a contribution of 97.01% (see Table 2). This behaviour can be explained by the deformation of the beam around the neutral axis, since the upper part of the beam itself is subjected to compressive stresses, while the bottom part is under tension. It was noted that cross-ply glass fibres retained a greater amount of matrix phase than unidirectional sisal fibres, which increases stiffness on the upper beam side under flexural loads. The transverse glass fibres may also provide additional reinforcement when subjected to the bending loading on the composite surface. In addition, the asymmetry of the fibre stacking sequence is responsible for modifying the equivalent flexural stiffness of the composites. This effect may hinder the mechanical behaviour of sisal fibres, especially in the compressive beam side.
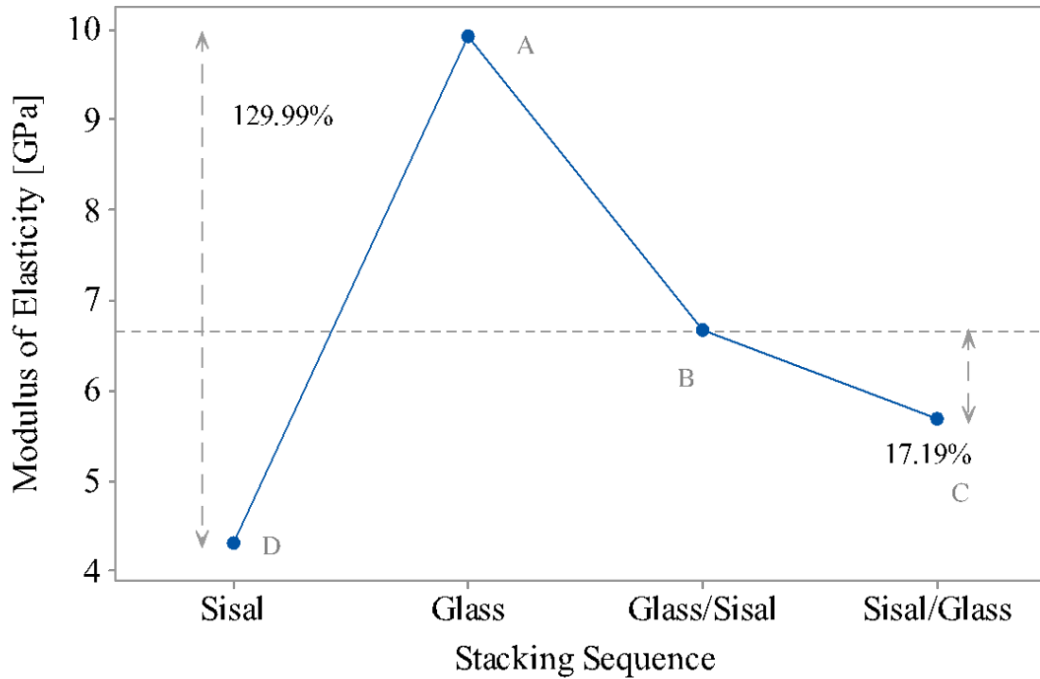
Figure 6. Main effect plot of the factor 'Stacking Sequence' related to the mean flexural modulus.

Figure 7 shows the effect of the inclusion of cement particles on the flexural modulus of the hybrid bio-composites. Laminates reinforced with 10wt% of cement particles present an increase of the flexural stiffness. In these cases, fracture during bending is induced by the compression at the top of the laminate. This feature suggests that the incorporation of cement particles, particularly inside the top side of the, tends to increase the compressive stiffness of the matrix, which results in an increment of the flexural modulus of the hybrid laminates. A similar behaviour is also observed by Detomi *et al.* [10]. In addition, a possible hydration of the cement grains by the epoxy polymer [30, 35] could contribute to increase the flexural stiffness, which can also be related to an improvement in the interfacial bonding inside the composite [37]. This matrix stiffening effect generated by the cement particles can enhance the resistance against interlaminar failure [20] and, consequently, increase the elastic modulus of the composite laminate.
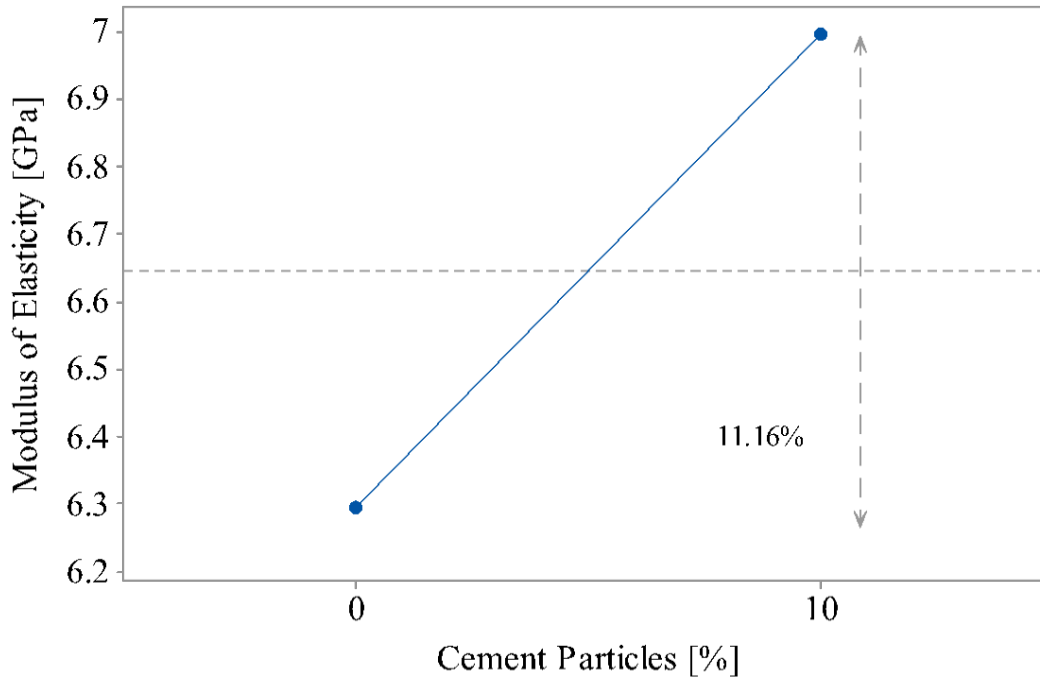
13

Figure 7. Main effect plot of the factor 'Cement Particles' associated to the mean flexural modulus.

3.5 Flexural Strength

The flexural strength of the hybrid reinforced composites ranges from 93.7 MPa to 333.7 MPa. The interaction between the stacking sequence and the dispersion of the cement particles is significant, with a P-value lower than 0.05 (see Table 2). The stacking sequence is however the most relevant design parameter affecting the flexural strength, with a contribution of 99.86%. Figure 8 shows the second order interaction effect plot for the flexural strength. In general, its behaviour is similar to that obtained for the flexural modulus presented in Figure 3. The bidirectional glass fibre layers located in the top side of the beam enhance the flexural strength of the hybrid composites. In contrast, glass fibres layers incorporated in the bottom beam side lead to a 58.75% reduction of flexural strength compared to the opposite arrangement set (Glass/Sisal). This behaviour can be attributed to the non-structural efficiency of sisal fibres under compressive loads.
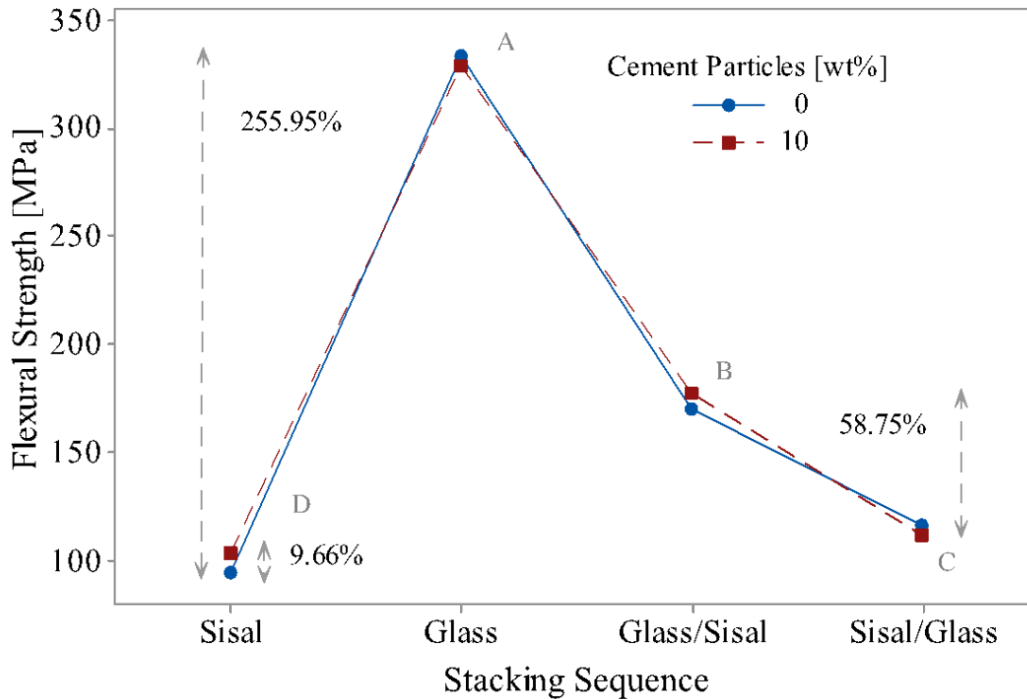
Figure 8. Interaction effect plot for the mean flexural strength.

3.6 Fracture analysis

Figure 9 shows a series of optical images related to glass/sisal fibres composites without (Figure 9a) and with cement (Figure 9b) inclusions. A brittle failure mode was most evident in these non-particulate composites (Figure 9a). The presence of cement particles contributes to enhance the stiffness of the matrix phase, especially under compressive loads on the upper side of the beam as reported by Melo *et al.* [26] and Torres *et al.* [27]. Although a delamination process is a common type of failure under flexural loading, this effect did not occur, indicating a good interfacial bonding, even when cement particles were used. The failure of the composites under flexural loading is mainly affected by the mechanical characteristics of the natural fibres, as reported by Belaadi *et al.* [39].
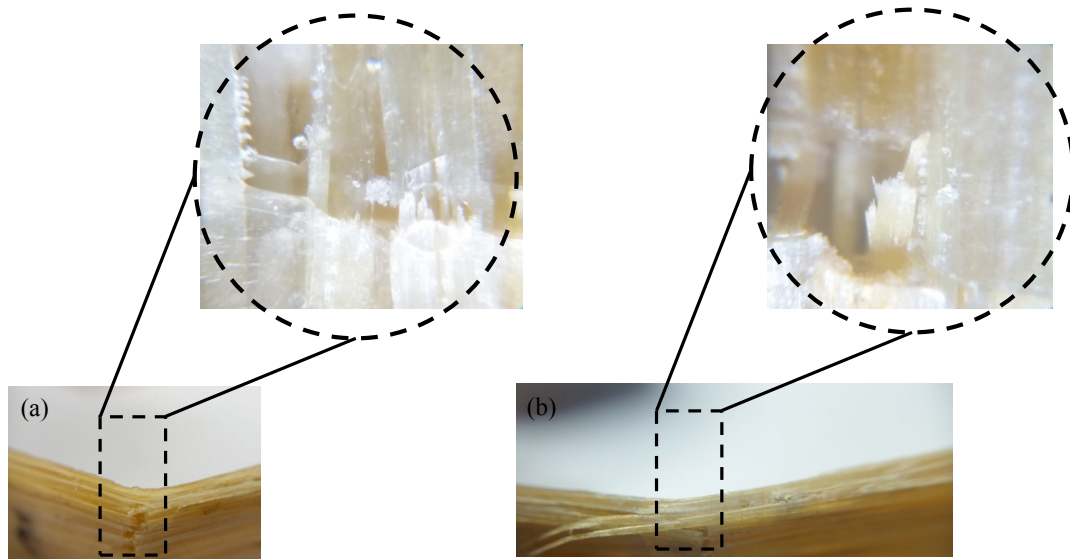
Figure 9. Fracture analysis of the glass-sisal reinforced composite without (a) and with cement microparticles (b)

Figure 10 shows that both sisal/glass (Figure 10a-b) and glass/sisal (Figure 10c-d) composites possess a brittle failure mode including, in some cases, a fibre pull-out effect. The failure mechanism of the hybrid composites is characterized by the presence of a partial rupture of the bottom layers. A major damage was observed in those composites without cement particles (Figure b-d). It is noteworthy that no delamination process was noted at the fibre interfaces. Figure 11 shows the mechanical behaviour of the hybrid composites under three-point bending test (Figure 11). Composites made with sisal fibres on the bottom beam side obtained higher flexural strength and a characteristic mode of brittle failure (Figure 10c-d). A fibre fraying effect was more evident in hybrid composites with glass fibres in the upper beam side. The cement particles led to increased toughness of the laminates, as shown in Figure 11. This behaviour can be attributed to the presence of particles in the interlaminar region, which contributes to retard crack propagation, as reported in literature [11, 26-27].
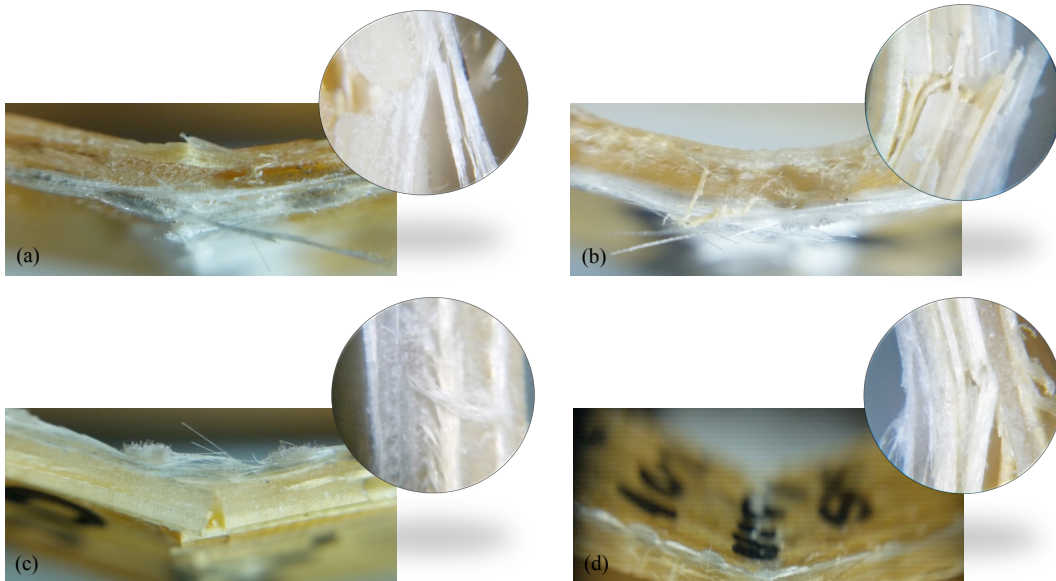
Figure 10. Fracture analysis of the hybrid sisal/glass (a-b) and glass/sisal (c-d) composite without (b-d) and with cement inclusions (a-c).
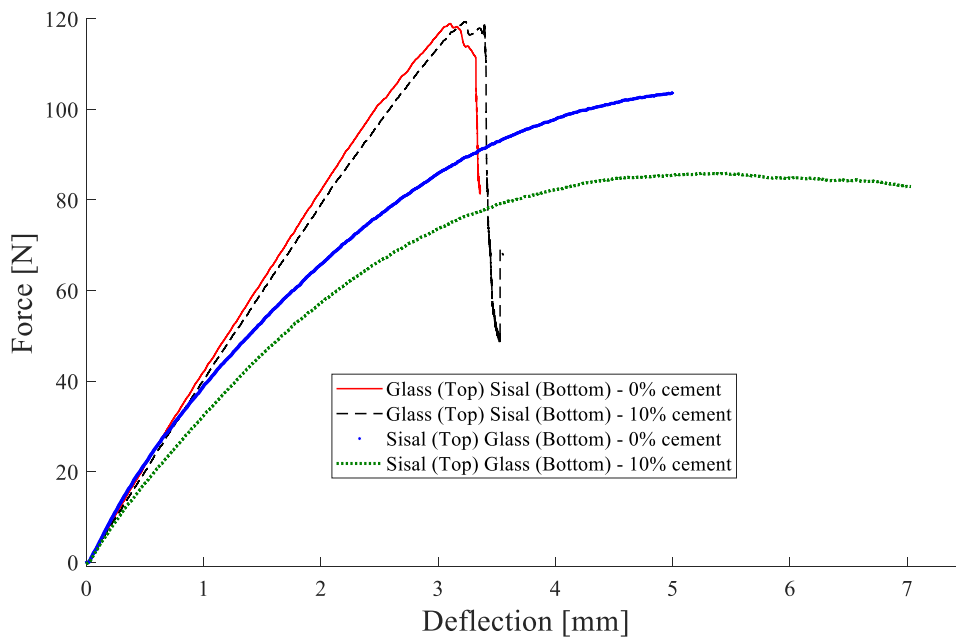

Figure 11. Flexural behaviour of the hybrid laminates.

The fractured surface of sisal fibre composites revealed substantial fibre pull-out effects (Figure 12a) relative to glass fibre composites (Figure 12b) attributed to lower fibre-matrix interaction.
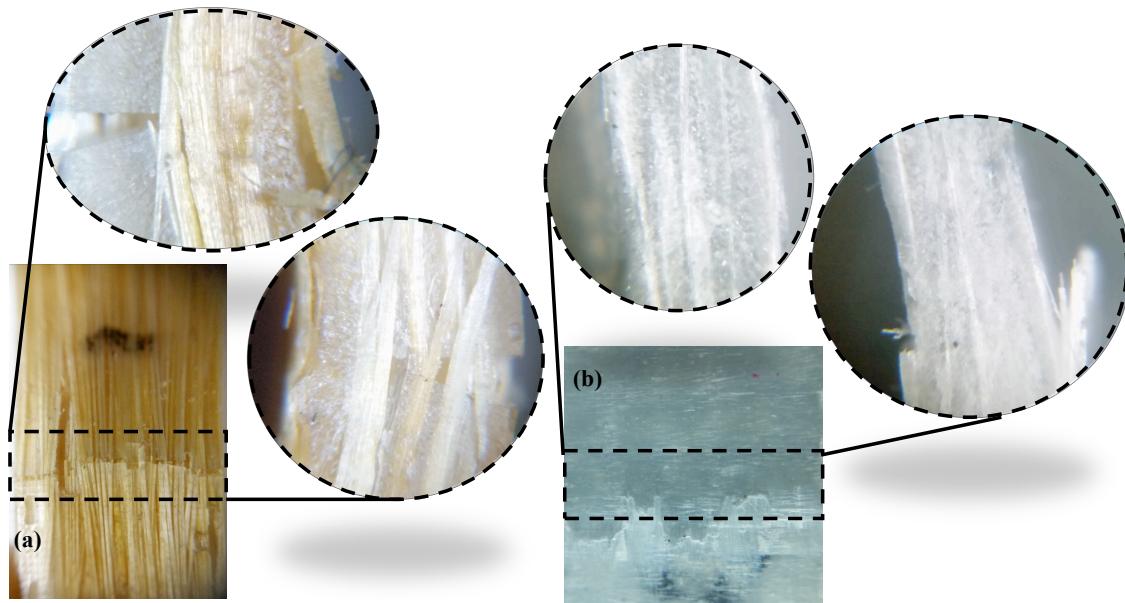
Figure 12. Fracture analysis of the unidirectional sisal fibre (a) and cross-ply glass fibre (b) composites without cement inclusions.

4. CONCLUSIONS

Sustainable hybrid composites based on sisal and glass fibres containing Portland cement inclusions have been designed and characterized. The main conclusions of this work are the following:

i. The fibre stacking sequence is the most relevant factor affecting the physical and mechanical properties of the hybrid bio-reinforced composites. This is particularly true for the flexural strength and stiffness, with 98% of contribution;

ii. In general, the presence of Portland cement increases the stiffness, apparent density, apparent porosity and water absorption of the composites;

iii. The stacking sequence significantly affected the flexural strength, apparent density, apparent porosity and water absorption responses.

iv. The failure mode of the hybrid composites consists of cracks in the matrix and fibre pull-out effects, especially when the natural fibres are incorporated. No delamination process was clearly identified in the hybrid composites, and that shows the presence of a good interfacial bonding between phases.

v. Cement particles led to increased toughness of the hybrid laminates.

vi. Finally, hybrid composites manufactured by the glass/sisal layout and 10wt% cement particles achieved the highest flexural strength and stiffness; this

configuration appears to provide promising properties for sustainable structural applications.

ACKNOWLEDGMENT

REFERENCES

[1]   T. Gurunathan, S. Mohanty, S. K. Nayak, A review of the recent developments in biocomposites based on natural fibres and their application perspectives. Composites Part A: Applied Science and Manufacturing, v. 77, (2015), pp. 1-25.

[2]   H. Dahy, Biocomposite materials based on annual natural fibres and biopolymers – Design, fabrication and customized applications in architecture. Construction and Building Materials, v. 147, (2017), pp. 212-220.

[3]   M.R. Sanjay, B Yogesha, Studies on Natural/Glass Fibre Reinforced Polymer Hybrid Composites: An Evolution, Materials Today: Proceedings, v. 4, (2017), pp. 2739-2747.

[4]   B. KC, O. Faruk, J.A.M. Agnelli, A.L. Leao, J. Tjong, M. Sain, Sisal-glass fibre hybrid biocomposite: Optimization of injection molding parameters using Taguchi method for reducing shrinkage. Composites Part A: Applied Science and Manufacturing, v. 83, (2016), pp. 152-159.

[5]   L.J. Silva, T.H. Panzera, V.R. Velloso, *et al.*, Hybrid polymeric composites reinforced with sisal fibres and silica microparticles, *Composites: Part B*, v. 43, (2012), pp. 3436-3444.

[6]   P. Rosso, L. Ye, K. Friedrich, K., *et al.*, A toughened epoxy resin by silica nanoparticle reinforcement, *Journal of Applied Polymer Science*, v. 100, n. 3, (2006), pp. 1849-1855.

[7]   J. Tsai., H. Hung, Y. Cheng, Investigating Mechanical Behaviors of Silica Nanoparticles Reinforced Composites. Journal of Composites Materials, v. 44, (2010), pp. 505-524.

[8] Andrew N. Rider, Qi An, Narelle Brack, Erik T. Thostenson, Polymer nanocomposite – fibre model interphases: Influence of processing and interface chemistry on mechanical performance, Chemical Engineering Journal, v. 269, (2015), pp. 121-134.

[9] J.C. Santos, L.M.G. Vieira, T.H. Panzera, M.A. Schiavon, A.L. Christoforo, F. Scarpa, Hybrid glass fibre reinforced composites with micro and poly-diallyldimethylammonium chloride (PDDA) functionalized nano silica inclusions, Materials & Design (1980-2015), v. 65, (2015), pp. 543-549.

[10] A.C. Detomi, R.M. Santos, S.L.M. Ribeiro Filho, C.C. Martuscelli, T.H. Panzera, F. Scarpa, Statistical effects of using ceramic particles in glass fibre reinforced composites, Materials & Design, v. 55, (2014), pp. 463-470.

[11] Y. Cao, J. Cameron. Impact Properties of Silica Particle Modified Glass Fibre Reinforced Epoxy Composite. Journal of Reinforced Plastics and Composites, v. 25, (2006), pp.761-769.

[12] J.S. Jang, et al. Experimental and analytical investigation of mechanical damping and CTE of both SiO2 particle and carbon nanofiber reinforced hybrid epoxy composites. Composites Part A: Applied Science and Manufacturing, v. 42, (2011), pp. 98-103.

[13] V.C.S. Chandrasekaran, S.G. Advani, M.H. Santare, Role of processing on interlaminar shear strength enhancement of epoxy/glass fiber/multi-walled carbon nanotube hybrid composites. Carbon. V. 48, (2010), pp.3692-3699.

[14] A. Ruggiero, P. Valasek, M. Müller, Exploitation of waste date seeds of Phoenix dactylifera in form of polymeric particle biocomposite: Investigation on adhesion, cohesion and wear, Composites Part B, v.104, (2016), pp. 9-16.

[15] S. Panthapulakkal, L. Raghunanan, M. Sain, B. KC, J. Tjong, Natural fibre and hybrid fibre thermoplastic composites: Advancements in lightweighting applications, Green Composites (Second Edition), (2017), pp. 39-72.

[16] Omar Faruk, Andrzej K. Bledzki, Hans-Peter Fink, Mohini Sain, Biocomposites reinforced with natural fibres: 2000–2010, Progress in Polymer Science, v. 37, (2012), pp. 1552-1596.

[17] Elaine C. Ramires, Jackson D. Megiatto, Christian Gardrat, Alain Castellan, Elisabete Frollini, Biobased composites from glyoxal–phenolic resins and sisal fibres, Bioresource Technology, v. 101, Issue 6, (2010), pp. 1998-2006.

[18] A.R. Martin, M.A. Martins, L.H.C. Mattoso, O.R.R.F. Silva, Chemical and structural characterization of sisal fibres from Agave sisalana variety, Polímeros, v. 19(1), (2009), pp. 40-46.

[19] C.A. Angrizani, C.A.B. Vieira, A.J. Zattera, E. Freire, R.M.C. Santana, S.C. Amico, Influência do comprimento da fibra de sisal e do seu tratamento químico nas propriedades de compósitos com poliéster, 17º CBECIMat - Congresso Brasileiro de Engenharia e Ciência dos Materiais, Foz do Iguaçu, PR, Brasil, Novembro 2006.

[20] L. M. G. Vieira, J. C. Santos, T. H. Panzera, A. L. Christoforo, V. Mano, J. C. Campos Rubio, F. Scarpa, Hybrid composites based on sisal fibres and silica nanoparticles. Polym. Compos. 2016, doi:10.1002/pc.23915.

[21] M.R. Sanjay, G.R. Arpitha, B. Yogesha, Study on Mechanical Properties of Natural - Glass Fibre Reinforced Polymer Hybrid Composites: A Review, Materials Today: Proceedings, v. 2, (2015), pp. 2959-2967.

[22] A. Padanattil, J. Karingamanna, Mini K.M., Novel hybrid composites based on glass and sisal fiber for retrofitting of reinforced concrete structures, Construction and Building Materials, v. 133, (2017), pp. 146-153.

[23] B. KC, O. Faruk, J.A.M. Agnelli, A.L. Leao, J. Tjong, M. Sain, Sisal/glass fiber hybrid biocomposite: Optimization of injection molding parameters using Taguchi method for reducing shrinkage, Composites: Part A (2015), doi: http://dx.doi.org/10.1016/j.compositesa.2015.10.034.

[24] M. Aslan, M. Tufan, T. Küçükömeroğlu, Tribological and mechanical performance of sisal-filled waste carbon and glass fibre hybrid composites, Composites Part B (2018), doi: 10.1016/j.compositesb.2017.12.039.

[25] F. M. Santos, F. B. Batista, T. H. Panzera, A. L. Christoforo, J. C. C. Rubio, Hybrid composites reinforced with short sisal fibres and micro ceramic particles. Matéria (Rio de Janeiro), v. 22, Issue 2, (2017), e-11838.

[26] A.B.L. Melo, T.H. Panzera, R.T.S. Freire, F. Scarpa, The effect of Portland cement inclusions in hybrid glass fibre reinforced composites based on a full factorial design, Composite Structures, doi: 10.1016/j.compstruct.2018.01.069.

[27] R.B. Torres, J.C. Santos, T.H. Panzera, A.L. Christoforo, P.H.R. Borges, F. Scarpa, Hybrid glass fibre reinforced composites containing silica and cement microparticles based on a design of experiment, Polymer Testing, v. 57, (2017), pp. 87-93.

[28] A.B.L. Melo, L.F.L. Paiva, J.C. Santos, T.H. Panzera,; R. T. S. Freire, A Statistical Analysis of Epoxy Polymer Reinforced with Micro Ceramic Particles. Journal of Research Updates in Polymer Science, v. 5, (2016), pp. 108-113.

[29] D. C. Montgomery. Design and analysis of experiments. 6ª edition. Arizona: John Wiley & Sons, Inc., 2005.

[30] C. F. J. Wu, M. Hamada, Experiments: planning, analysis, and parameter design optimization. New York: John Wiley & Sons, 2000.

[31] American Society for Testing and Materials. ASTM D790-15e1, Standard Test Methods for Flexural Properties of Unreinforced and Reinforced Plastics and Electrical Insulating Materials, ASTM International, West Conshohocken, PA, (2015), doi:10.1520/D0790-15E01.

[32] American Society for Testing and Materials. ASTM D792-13, Standard Test Methods for Density and Specific Gravity (Relative Density) of Plastics by Displacement, ASTM International, West Conshohocken, PA, (2013), doi:10.1520/D0792.

[33] British Standards Institution. BS EN ISO 10545-3:1997. Part 3: Determination of Water Absorption, Apparent Porosity, Apparent Relative Density and Apparent Density. BSI, London (1997), doi:10.3403/01217243U.

[34] T.H. Panzera, A.L.R. Sabariz, K. Strecker, P.H.R. Borges, D.C.L. Vasconcelos, W. L. Wasconcelos, Mechanical properties of composite materials based on Portland cement and epoxy resin. Cerâmica, v. 56, (2010) pp. 77-82.

[35]   C.C. Martuscelli, J.C. Santos, P.R. Oliveira, T.H. Panzera, M.T.P. Aguilar, C.T. Garcia, Polymer-cementitious composites containing recycled rubber particles, Construction and Building Materials, v. 170, (2018), pp. 446-454.

[36]   C. Soles, A. Yee. A discussion of the molecular mechanisms of moisture transport in epoxy resins. Journal of Polymer Science, Part B: Polymer Physics, v. 38, (2000), pp. 792–802.

[37]   P.A. Sreekumar, S.P. Thomas, J.M. Saiter, K. Joseph, G. Unnikrishnan, and S. Thomas, Effect of fiber surface modification on the mechanical and water absorption characteristics of sisal/polyester composites fabricated by resin transfer molding. Compos. A Appl. Sci. Manufact., v. 40, (2009), pp. 1777-1784.

[38]   C.M. Manjunatha, A.C. Taylor, A.J. Kinloch, and S. Sprenger, The effect of rubber micro-particles and silica nano-particles on the tensile fatigue behaviour of a glass-fibre epoxy composite, J. Mater. Sci., v. 44, (2009), pp. 342-345.

[39]   A. Belaadi, A. Bezazi, M. Bourchak, F. Scarpa, Tensile static and fatigue behaviour of sisal fibres. Materials and Design, v. 46, (2013), pp. 76–83.